Theoretical Study of Intermolecular Potential Energy Surface for HCl Dimer: Example of Nonspherical Atom–Atom Exchange Repulsion Interaction

JOSE M. HERMIDA-RAMÓN,[1] OLA ENGKVIST,[2] GUNNAR KARLSTRÖM[2]

[1]*Department of Physical Chemistry, University of Santiago de Compostela, Santiago de Compostela, Spain*
[2]*Department of Theoretical Chemistry, University of Lund, P.O.B. 124, S-221 00 Lund, Sweden*

Received 18 November 1997; accepted 13 July 1998

ABSTRACT: The intermolecular part of the potential energy surface for the HCl dimer has been studied with *ab initio* quantum chemical methods. An intermolecular potential, based on quantum chemical calculations has been constructed. The interaction energy consists of electrostatic, induction, and dispersion terms calculated from the monomer properties of the interacting molecules and an exchange repulsion term. The latter term was parameterized from the results of the quantum chemical calculations and estimates of the electrostatic and induction energies. It was found necessary to use nonspherical atom–atom exchange repulsion interaction parameters, and the parameters describing the deviation from spherical behavior could be obtained from the expectation values of r^2 for the electrons assigned to an atom. J Comput Chem 19: 1816–1825, 1998

Keywords: HCl dimer; intermolecular potential; nonspherical atom–atom exchange repulsion; virial coefficient; r^2 expectation values

Correspondence to: G. Karlström
Contract/grant sponsor: Santiago de Compostela University; Xunta de Galicia

CCC 0192-8651 / 98 / 161816-10

Introduction

The study of intermolecular interactions is one of the fields in which quantum chemical *ab initio* methods have made the largest contribution, both qualitatively and quantitatively, to our knowledge in chemistry. One of the standard procedures to construct an intermolecular potential between two rigid molecules is to perform supermolecule calculations for a large number of different complex geometries and fit the calculated interaction energies, to a suitable functional form. The interaction energies are usually corrected for basis set superposition error (BSSE).[1–3] Studies of this type have recently been published for the HCl dimer.[4, 5] A fundamental problem with this approach is that, because the functional form used generally does not contain any information about the properties of the interacting molecules, a large number of different geometries must be studied using the supermolecular approach. Furthermore, because each calculation may be rather time-consuming, the construction of intermolecular potentials using this approach may require significant computer resources, especially if the results are to be corrected for basis set superposition error.

To deal with these problems we have developed an alternative method to construct intermolecular potentials, which is based on the properties of the interacting molecules. The method has been given the name NEMO.[6–9] The starting point for this approach is **one** quantum chemical *ab initio* calculation on each of the interacting molecules. The charge distributions of the molecules are partitioned into a multicenter multipole expansion.[10, 11] The molecular polarizability is, in a similar way, divided into local contributions.[12] Using these entities, it is possible to calculate electrostatic and induction interactions between molecules using classical electrostatics. Furthermore, using an empirically corrected version of London's dispersion energy formula,[12] one may obtain an estimate of the dispersion interaction between the molecules. The remaining part of the interaction energy is dominated by the exchange repulsion, and, in the NEMO approach, this term has been parameterized by using the overlap between the wave functions of the interacting molecules. In a second step, these repulsion energies are fitted to a function, which is exponential over interatomic distances and easier to evaluate. The drawback of this ansatz is that, for each geometry considered, one needs to calculate the overlap integrals between the interacting molecules. This require considerably reduced computer resources than ordinary supermolecular *ab initio* calculations, but it is still the bottleneck in the NEMO approach. In this work, we will instead investigate the possibility of directly fitting the exponential function to the exchange repulsion energies, but at the same time incorporate information obtained from the *ab initio* calculations on the individual molecules.

The HCl dimer has previously been studied extensively. Both accurate *ab initio* calculations[4, 5, 14–18] and high quality experimental investigations[19–21] have been performed to study the intermolecular potential energy surface. The main purpose of this work is not to construct an intermolecular potential for the HCl dimer of higher quality than that of already existing ones, but instead to investigate the reliability of a new method to model the short range repulsive forces between molecules.

The outline of the remainder of this article is that, in the next section, we briefly give the mathematical formulation of the standard NEMO method; the third section will deal with the modified repulsive interaction; and the last section will be used to describe the potentials obtained.

NEMO Method

In the Introduction we briefly discussed the construction of intermolecular potentials. In the NEMO method, which is a compromise between computational efficiency and reliability of the resulting potential, the total interaction energy between two molecules is constructed from four different energy contributions, each with its own physical interpretation:

$$E_{\mathrm{tot}} = E_{\mathrm{ele}} + E_{\mathrm{ind}} + E_{\mathrm{disp}} + E_{\mathrm{exrep}} \qquad (1)$$

Here, E_{tot} is the total interaction energy, E_{ele} is the electrostatic energy, E_{ind} the inductive energy, E_{disp} the dispersion energy, and E_{exrep} is the interaction energy at the HF level, which is not included in the electrostatic and induction terms. The largest contribution to the E_{exrep} term arises from the exchange repulsion energy, whereas smaller contributions originate from charge transfer and different coupling terms. In the NEMO model, the first three of these contributions are calculated from information obtained from *ab initio* quantum

chemical calculations on each of the interacting molecules. There are two important advantages with this approach relative to supermolecular calculations: First, the method gives a clear separation between the three energy contributions that are almost pairwise additive and the induction energy that specifies a real many-body contribution for a many-particle system. Second, the computationally demanding quantum chemical calculations are only required once for each of the interacting molecules. The basis set superposition error is avoided automatically in the NEMO scheme. In what follows we describe how each of the energy contributions to the interaction energy is calculated and then discuss the construction of the interaction potential.

The starting point of our discussion is that a Hartree–Fock (HF) calculation is performed for the HCl molecule. Here, quantum chemical calculation was performed with the MOLCAS-2 package,[22] using an atomic natural orbitals (ANO) basis set. For third row atoms, like chlorine, a (13s8p3d) primitive basis set was contracted to (6s5p1d) and, for hydrogen, a (6s4p) primitive basis set was contracted to (3s2p).[23] In Table I we present the molecular geometry used and the calculated dipole moment, quadrupole moment, and polarizability tensor.

The orbitals from the HF calculations can be analyzed as follows. A HF wave function can be written as an expansion of a set of orbitals. These orbitals are constructed from a set of basis functions:

$$\psi_i = \sum_\mu c_{i\mu}\,\chi_\mu \tag{2}$$

where ψ_i is an orbital, $c_{i\mu}$ an orbital coefficient, and χ_μ a basis function centered at a nucleus. The density matrix, D, is defined as:

$$D_{\mu\nu} = \sum_i n_i c_{i\mu} c_{i\nu} \tag{3}$$

where n_i is the occupation number.

TABLE I.
Monomer SCF Results (in Atomic Units).

	ANO	Experimental
rCl—H	2.4085	2.4086[a]
μ	0.4655	0.4301[b]
Q	2.91	2.78[c]
$P_\parallel$	17.35	18.70[d]
$P_\perp$	14.22	16.74[d]

[a]Ref. 28. [b]Ref. 29. [c]Ref. 30. [d]Ref. 29 and 31.

The total molecular charge distribution may be expanded as:

$$\rho = \sum_\mu \sum_\nu D_{\mu\nu}\,\chi_\mu\,\chi_\nu \tag{4}$$

If we use the fact that the basis functions are centered at the nuclei, it is possible to divide the charge distribution into local contributions, ρ_{kl}, where k and l are nuclei:

$$\rho_{kl} = \sum_{\mu\in k} \sum_{\nu\in l} D_{\mu\nu}\,\chi_\mu\,\chi_\nu \tag{5}$$

A local charge for each pair of atoms can thus be calculated from:

$$q_{kl} = \sum_{\mu\in k} \sum_{\nu\in l} D_{\mu\nu}\langle\,\chi_\mu|\,\chi_\nu\rangle \tag{6}$$

In a similar way, it is possible to define local dipole moments, quadrupole moments, and higher order moments by replacing the overlap integral in eq. (6) with a dipole or higher order moment integral. The nuclear charges are conveniently added to the diagonal charges, q_{kk}. A complete description of this procedure is given elsewhere.[10] The method is very similar to distributed multipole analysis (DMA),[24] developed somewhat later.

From knowledge of the charge distribution of the HCl molecule it is possible to calculate the electrostatic interaction between two HCl molecules. A weak point in this procedure is that corrections to the electrostatic interaction, due to the overlap of the two charge distributions, are ignored. We will discuss this point further in connection with the exchange repulsion interaction.

To calculate the induction interaction, we need, apart from the description of the charge distributions just discussed, a distributed representation of the molecular polarizability. Such a scheme for dividing the molecular polarizability into local contributions within the uncoupled HF approximation has previously been devised by one of us.[12] One component of the polarization tensor can, within this approximation, be written as:

$$P_{xx'} = 4\sum_i \sum_j \langle\psi_i|x|\psi_j\rangle\langle\psi_i|x'|\psi_j\rangle/(\varepsilon_j - \varepsilon_i) \tag{7}$$

where ψ_i is an occupied orbital and ψ_j is an unoccupied orbital, and ε_i and ε_j are the corresponding orbital energies. If an expansion of the orbitals, according to eq. (2), is inserted into eq. (7), one obtains an expression for the polarizability,

which involves a four-index summation over basis functions:

$$P_{xx'}^{klmn} = 4\sum_{i,j}\frac{1}{\varepsilon_j - \varepsilon_i}\sum_k\sum_{\mu_k}\sum_l\sum_{\nu_l}\sum_m\sum_{\sigma_m}\sum_n\sum_{\tau_n} C_{i\mu_k} \times C_{j\nu_l}C_{i\sigma_m}C_{j\tau_n}\langle \chi_{\mu_\kappa}|x|\chi_{\nu_i}\rangle\langle \chi_{\sigma_m}|x'|\chi_{\tau_n}\rangle \quad (8)$$

Two of these summations are over occupied orbitals and two are over virtual orbitals. Normally, the virtual orbitals are diffuse and, when the summation is performed over these, one obtains:

$$P_{xx'}^{km} = \sum_l\sum_n P_{xx'}^{klmn} \quad (9)$$

Using a similar technique as the one used to create the multicenter multipole expansion just described it is now possible to calculate the local contribution to the molecular polarizability. Formally, the result will depend on the expansion center, and each contribution to the total molecular polarizability is expanded around an origin[12] defined according to:

$$R_{ij} = 0.5*(R_i + R_j) \quad (10)$$

where R_i is the center of charge for orbital i. In Table II we show the sites and their electrostatic properties, as calculated for the HCl molecule using the orbitals obtained from the HF calculation on the HCl molecule.

In the NEMO model, the dispersion is calculated using a London-type formula[13]:

$$E_{\text{disp}} = \sum_{mn}^{\substack{\text{atom centers}\\ \text{bond centers}}} f_{mn}(CE_{12}/4)\sum_{ijkl}^{3} P_{ij}^m P_{kl}^n T_{ik}T_{jl} \quad (11)$$

where P_{ij}^m is a component of the local polarizability tensor at center m, T_{ik} a component of the interaction tensor $\vec{\nabla}\vec{\nabla}(\frac{1}{r})$, C a correction factor (with the value of 1.89) obtained from calculations on small dimer complexes with Møller–Plesset second order perturbation theory (MP2),[25] and E_{12} the average molecular ionization energy defined according to:

$$E_{12} = \frac{E_1 E_2}{E_1 + E_2} \quad (12)$$

Here, E_1 is the ionization energy for molecule 1 and E_2 the ionization energy for molecule 2. The damping function, f_{mn}, corrects for overlap effects of the charge distributions.[9,26]

Using a perturbation approach one can show that the exchange repulsion interaction between

TABLE II.
Coordinates, Charges, Dipole Moments, Quadrupole Moments, and Polarizabilities for HCl Models (All Values in Atomic Units).

Model	Two-Center Model		Three-Center Model		
Center	Cl	H	Cl	H	C. of Bond
x	0.00	0.00	0.00	0.00	0.00
y	0.00	0.00	0.00	0.00	0.00
z	−0.0688	2.3397	−0.0688	2.3397	1.0928
q	−0.1255	0.1255	0.2112	0.4391	−0.6503
μ_x	0.00	0.00	0.00	0.00	0.00
μ_y	0.00	0.00	0.00	0.00	0.00
μ_z	0.3743	−0.2108	0.6906	0.0839	−0.6111
Q_{xx}	−9.8883	−0.6360	−9.6447	−0.4091	−0.4706
Q_{yy}	−9.8883	−0.6360	−9.6447	−0.4091	−0.4706
Q_{zz}	−7.2122	−0.0523	−7.5277	−0.4106	−0.2680
Q_{xy}	0.00	0.00	0.00	0.00	0.00
Q_{xz}	0.00	0.00	0.00	0.00	0.00
Q_{yz}	0.00	0.00	0.00	0.00	0.00
P_{xx}	12.9786	1.2435	12.2637	0.5286	1.4299
P_{yy}	12.9786	1.2435	12.2637	0.5286	1.4299
P_{zz}	12.8863	4.4636	10.9970	2.5743	3.7786
P_{xy}	0.00	0.00	0.00	0.00	0.00
P_{xz}	0.00	0.00	0.00	0.00	0.00
P_{yz}	0.00	0.00	0.00	0.00	0.00

two molecules is proportional to the square of the overlap between the monomer wave functions (S^2) at large distances.[27] In the standard NEMO model, we have for shorter distances, chosen to model this term by a power series expansion according to $\alpha S^2 + \beta S^4 + \gamma S^6 + \cdots$. Note that odd terms cannot appear in the expansion. The exchange repulsion also depends on the nature of the interaction molecules. If the overlapping electronic clouds are easy to polarize and weakly bound to the system, then one can expect the exchange repulsion to be weak, and, in the opposite case, to be strong. To take these effects into account we have introduced a set of atom pair parameters α, β, and γ, which depends on the types of interacting atoms[6]:

$$E_{\text{rep}} = \sum_{m,n}^{\text{atoms}} \alpha_{mn}\Theta_{mn} + \beta_{mn}\Theta_{mn}^2 + \gamma_{mn}\Theta_{mn}^3 \quad (13)$$

Θ is defined as:

$$\Theta_{mn} = \sum_{i_m k_n}^{\text{orb}} \frac{-\varepsilon_i \varepsilon_j}{\varepsilon_i + \varepsilon_j} O_{ik} \sum_{j_m j_n}^{\text{basfun}} c_{i_m j_m} c_{k_m j_n} S_{j_m j_n} \quad (14)$$

where ε_i and ε_j are orbital energies. O_{ik} is the orbital overlap, defined as:

$$O_{ik} = \sum_{p}^{\text{atoms}} \sum_{q}^{\text{atoms}} \sum_{j_p}^{\text{basfun}} \sum_{j_q}^{\text{basfun}} c_{i_p j_p} c_{k_q j_q} S_{j_p j_q} \quad (15)$$

where c_{ij} is an orbital coefficient and S_{mn} is the overlap integral between basis functions (bas fun) m and n. Factors α, β, and γ in eq. (13) are fitted from SCF calculations on small dimer complexes.[6] For these complexes we define the exchange repulsion energy as:

$$E_{\text{rep}} = \Delta E_{\text{SCF}} - E_{\text{ele}} - E_{\text{ind}} \quad (16)$$

where ΔE_{SCF} is the interaction energy at the SCF level. The BSSE is corrected for with the full counterpoise correction.[1,2] E_{ele} is the electrostatic interaction energy calculated with the multicenter multipole expansions of the two molecules, and E_{ind} the induction energy calculated with the multicenter multipole expansions and the local polarizabilities of the two molecules. With this definition, the exchange repulsion energy will not only contain the true exchange repulsion, but also overlap corrections to the electrostatic and induction interaction as well as the charge transfer interaction. All these terms depend on the overlap between the wave functions of the two molecules, motivating the choice of model for the exchange repulsion energy, as follows. Using Eqs. (13) and (16), optimal values for the α, β, and γ parameters are determined. To calculate the exchange repulsion interaction for a given geometry and provided that the parameters α, β, and γ have been independently determined, one thus needs to evaluate a set of overlap integrals for that particular geometry. This is rather time-consuming and, to be of any use in molecular simulation work, the exchange repulsion energies thus calculated are fitted to an expression of the following type:

$$E^{\text{rep}} = \sum_{m}^{\text{atom in mol 1}} \sum_{n}^{\text{atoms in mol 2}} f_{mn} e^{-g_{mn} r_{mn}} + \left(\frac{h_{mn}}{r_{mn}}\right)^q \quad (17)$$

In eq. (17), f_{mn}, g_{mn}, and h_{mn} are parameters depending on the atoms m and n, and q is an integer normally assigned a value of 20. (The last term, depending on h_{mn}, is a short-range term introduced to ensure that the repulsive energy dominates over the attractive electrostatic, inductive, and dispersive terms at short distances and prevents the total energy from approaching large negative values for small internuclear separations.) An unfortunate feature of an expression that of eq. (17) is that atom–atom repulsion interactions are spherical. In a recent publication by Meredith et al.[5] it was shown that, in particular, the Cl–Cl interaction in the HCl dimer is nonspherical. This naturally reflects the fact that the electrons are nonspherically distributed around the Cl atom in the HCl molecule.

Because all energy contributions included in the exchange-repulsion term can be represented by an exponential expression, it is tempting to fit this term with an exponential expression like eq. (17). To make such a fit we calculated the HF energy in a total of 62 different points of the HCl dimer surface. It could be contended that the number of points we explored was too small; however, because we fit only the most short-ranged component of the intermolecular interaction energy and not the total intermolecular energy, as was done when the supermolecule method was used, we were convinced that it was not necessary to make so many calculations as for the standard supermolecule scheme. Among these 62 points, we included points around the minimum and the main transition state; we also included points with linear configurations. In general terms, the choice of points was guided by our chemical intuition to explore the regions considered most important, so

that the interpolation function should properly describe the exchange-repulsion energy.

Because a chlorine atom in a molecule is nonspherical, it is important to take into account the anisotropy in the repulsion model for chlorine-containing molecules. For this reason we introduced a method that uses an important part of the anisotropy. This is the part monitored by the anisotropy of the local charge distributions, as shown by the expectation values of r^2 of the local electronic charge density. By doing so, the energy arising from the previously calculated *ab initio* exchange repulsion term between two molecules, A and B, is written as:

$$E_{\text{rep}} = \sum_{m \in A}^{\text{atoms}} \sum_{n \in B}^{\text{atoms}} a_{mn} e^{-b_{mn} r_{mn}^{\text{rep}}} \tag{18}$$

where a_{mn} and b_{mn} are fitted coefficients and r_{mn}^{rep} is defined by:

$$r_{mn}^{\text{rep}} = \sqrt{Tr(Q_{mn})} * \sqrt{\vec{r}_{mn} A_{mn} \vec{r}_{mn}^{+}} \tag{19}$$

and A_{mn} is given by:

$$Q_{mn}^{-1} = A_{mn} \Rightarrow Q_{mn} * A_{mn} = 1 \tag{20}$$

and Q_{mn} is defined as:

$$Q_{mn} = Q_{A_m} + Q_{B_n} \Rightarrow Q_{kl}^{mn} = Q_{kl}^{A_m} + Q_{kl}^{B_n} \tag{21}$$

where $Q_{kl}^{A_m}$ and $Q_{kl}^{B_n}$ are the *kl* components of the local r^2 expectation-value tensor of the electrons assigned to center *m* at molecule A and center *n* at molecule B. Thus, we have used the inverse of this tensor as a metric matrix. The implication of this is that the apparent distances in directions where the electron clouds have a large extension becomes smaller than in other directions, resulting in a larger exchange-repulsion interaction.

Potential Models

The main purpose of this work is to investigate the reliability of different procedures to construct intermolecular potentials. This is obviously always a compromise between simplicity and accuracy. Normally users of intermolecular potentials are interested in reducing the number of sites used in the potential function. The standard number is the number of atoms in the molecule. In the NEMO approach, the description of the molecular charge and polarizability distributions is initially divided into atoms and bonds in the interacting molecules. In a later step there is a possibility to partition the charges, dipoles, and quadrupoles as well as the polarizabilities assigned to the bonds to the atoms forming the bonds. In practice, this means, for the HCl dimer, that there is the possibility to construct potentials with two or three sites in each molecule. Furthermore, we can use the anisotropy obtained from the r^2 matrices with two or three centers. This means that several different potentials can be constructed. It should also be noted that the description of the electrostatic is truncated after the dipole term. To ensure that the total molecular quadrupole moment of the HCl molecule is correct, it is necessary to slightly modify the local dipoles.

In Table III we present the mean error of different fits obtained using different methods. In all, 62 different dimer geometries were used in the fit. From Table III it is clearly seen that one of the two-center repulsion models is significantly better than the other two-center models. This is the model where the *Q* matrices are taken from the three-center electrostatic descriptions, but only the contributions for the two atoms are used, and where a full three-center description is also used to model electrostatic, induction, and dispersion interaction. When a less sophisticated description is used for either the electrostatic or for the exchange repulsion energies, then the quality of the fit is lower. All true three-center models are of the same quality. It should be noted, however, that the three-center anisotropic models were always easier to fit, and that, for fewer dimer configurations, the isotropic three-center models frequently resulted in formally good fits to the geometries used. When the potential energy surfaces obtained were analyzed, they frequently ''misbehaved'' in certain regions of space. This never happened for the anisotropic three-center models. In Table III we present the parameters *a* and *b* obtained in the different fits. In this table we label the potentials and specify the way the electrostatic and induction interactions were calculated as well as the way the exchange-repulsion interaction was parameterized. It should also be noted that some of the parameters in Table III were less well determined. This normally corresponds to a situation in which there is no influence from the poorly determined parameters on the potential energy surface obtained from the parameters. We have also tried even simpler models to describe the electrostatic interaction between the molecules; for instance, an electrostatic two-center description in which the local

TABLE III.
Parameters, Error and Weight for Different Exchange-Repulsion Energy Fits (a in kcal / mol and b in Bohr $^{-1}$).

Electrostatic Model	Two centers	Two centers	Three centers	Three centers	Three centers	Three centers	Three centers
Repulsion model	Isotropic two-center model	Anisotropic two-center model with two-center quadrupoles	Isotropic three-center model	Anisotropic three-center model with three-center quadrupoles	Isotropic two-center model	Anisotropic two-center model with two-center quadrupoles	Anisotropic two-center model with three-center quadrupoles
Potential label	A	B	C	D	E	F	G
$\mathbf{a}_{Cl-Cl}$	42045.468	249565.977	458858.014	51387.436820	106468.057	60671.789	78326.834
$\mathbf{a}_{Cl-H}$	13414.509	3739.195	33574.183	2616.954884	3195.018	1600.170	4288.978
$\mathbf{a}_{Cl-bond}$	—	—	11765.668	20104923762.5	—	—	—
$\mathbf{a}_{H-H}$	3164889378.54	0.000000131	2914917075.40	50332345203.1	9551055051.39	0.0000000378	166.605
$\mathbf{a}_{H-bond}$	—	—	51041.350	4720.256	—	—	—
$\mathbf{a}_{bond-bond}$	—	—	23972256467.6	2111712154.29	—	—	—
$\mathbf{b}_{Cl-Cl}$	1.613898	1.859111	2.124442	1.582885	1.763615	1.634502	1.647295
$\mathbf{b}_{Cl-H}$	1.870334	1.593903	2.320742	1.644052	1.556778	1.42161	1.722404
$\mathbf{b}_{Cl-bond}$	—	—	1.560303	5.023326	—	—	—
$\mathbf{b}_{H-H}$	23.580190	0.021629	7.674720	14.922475	27.501250	0.006147	1.195313
$\mathbf{b}_{H-bond}$	—	—	3.100512	1.998126	—	—	—
$\mathbf{b}_{bond-bond}$	—	—	14.655565	12.280060	—	—	—
Error	20.210532	12.743840	1.332732	1.181104	9.426951	13.875179	2.321270
Weight	92.678669	92.678669	84.642534	84.642534	84.642534	84.642534	84.642534

[a]The different models are specified according to electrostatic and exchange repulsion model and are labeled.

quadrupoles were completely ignored, and not incorporated in the local dipoles was of such low quality that we chose not to present it.

The main purpose of the present work is to investigate how different fitting procedures should be used to obtain good potential functions, but of course it is of interest to construct a potential that is as reliable as possible for the HCl dimer using the available data. The main error in an approach like the one presented here originates from the dispersion energy estimate. Because the basis set used was fairly limited, one may expect that the dispersion energy was underestimated.

We believe that we have underestimated the dispersion energies by roughly 20%. To correct this underestimation, we constructed a high-quality potential based on the three-center electrostatic and exchange repulsion (anisotropic) description, in which the dispersion energy estimates were multiplied by 1.2. We labeled this potential dispersion *scaled*. Tables IV and V present the energies and geometries of the stationary points found in the different potentials; Figure 1 shows the reference system used for definition of geometry parameters describing the stationary points; and, finally, in Table VI we present the virial coefficient calculated with the different potentials. Here it should be noted that the virial coefficients were calculated using classical mechanics and that one may expect the quantum effect to yield higher values for the experimentally observed virial coefficients at low temperatures.[33]

Conclusions

In this work, we have shown that use of the local r^2 expectation values obtained from the molecular electronic wave function may improve the description of the intermolecular exchange repulsion in intermolecular potentials. In particular, we note that the anisotropy obtained in this way is similar to that obtained from fitting to *ab initio* data.[5] We have also demonstrated that an intermolecular potential for the HCl dimer obtained

TABLE IV.
Comparison with Previously Selected Calculations of $(HCl)_2$ for C_S Conformation—Binding Energies and Geometries (All Points Have $\phi = 180.0°$).

	Method	E_{tot} (kJ mol^{-1})	R (bohr)	θ_1 (°)	θ_2 (°)
Tao and Klemperer[4]	MP2	−8.49	7.145	8.0	90.0
Tao and Klemperer[4]	MP4	−7.69	—	—	—
Karpfen et al.[13]	ACPF[a]	−7.20	7.329	7.2	88.4
Karpfen et al.[13]	ACPF[b]	−7.03	7.281	6.6	88.0
Votava et al.[14]	CEPA	−7.94	7.228	2.5	82.5
Elrod and Saykally[19]	Semiempirical	−8.28	7.079	9.0	89.8
Bunker et al.[15]	Analytical fit	−7.49	7.219	7.4	87.7
Latajka et al.[16]	MP2	−6.63	7.189	11.9	89.1
Muenter[17]	Semiempirical	−5.61	7.276	−15.0	93.0
Meredith et al.[5]	L–J model	−9.163	7.030	5.7	82.9
Meredith et al.[5]	Anisotropic exp. 6 model	−8.18	7.238	12.9	84.4
This work	A	−9.73	7.081	4.2	83.6
This work	B	−8.99	6.945	−4.6	64.3
This work	C	−8.31	7.151	5.5	93.4
This work	D	−7.20	7.200	0.8	73.8
This work	D dispersion scaled	−8.44	7.056	0.4	71.9
This work	E	−6.63	7.207	20.7	102.3
This work	F	−5.54	7.391	−2.3	68.3
This work	G	−6.76	7.311	2.5	76.5
Novick et al.[20] Pine et al.[20]	Experimental	−9.50 ± 1.03	6.803	0.0	90.0
Schuder et al.[21]	Experimental	—	—	16.0	87.0

[a]Basis set (13s10p4d/6s2p) contracted to [6,5,2/4,2].
[b]Basis set (13s10p4d1f/6s2p) contracted to [6,5,3,1/4,2].

TABLE V.
Comparison with Previously Selected Calculations of $(HCl)_2$ for C_{2h} Conformation—Binding Energies and Geometries (All Points Have $\phi = 180.0°$).

	Method	E_{tot} (kJ mol^{-1})	R (bohr)	θ_1 (°)	θ_2 (°)
Tao and Klemperer[4]	MP2	−7.79	6.954	46.0	134.0
Tao and Klemperer[4]	MP4	−7.14	—	—	—
Karpfen et al.[13]	ACPF[a]	−6.28	7.196	48.0	132.0
Karpfen et al.[13]	ACPF[b]	−6.02	7.155	47.6	132.4
Votava et al.[14]	CEPA	—	—	—	—
Elrod and Saykally[19]	Semiempirical	−7.69	6.898	47.0	133.0
Bunker et al.[15]	Analytical fit	−6.72	7.194	47.2	132.8
Latajka et al.[16]	MP2	−6.09	6.984	51.4	128.6
Muenter[17]	Semiempirical	−5.37	—	—	—
This work	A	−6.95	6.828	54.1	125.9
This work	B	−5.85	7.071	47.0	133.0
This work	C	−6.06	7.159	46.4	133.6
This work	D	−6.41	7.076	46.5	133.5
This work	D dispersion scaled	−7.36	7.004	37.2	124.2
This work	E	−6.62	6.955	48.4	131.6
This work	F	−6.39	6.851	40.5	139.5
This work	G	−6.25	6.959	47.2	132.8

[a]Basis set (13s10p4d/6s2p) contracted to [6,5,2/4,2].
[b]Basis set (13s10p4d1f/6s2p) contracted to [6,5,3,1/4,2].

TABLE VI.
Second Virial Coefficients for Different Temperatures.

T (K)	Experimental[a]	A	B	C	D	D Dispersion Scaled with 1.2	E	F	G
175	—	−887.7	−676.5	−560.5	−446.5	−763.4	−379.7	−298.9	−392.8
190	−456.0	—	—	—	—	—	—	—	—
200	−392.0	−528.5	−426.3	−362.0	−296.5	−481.2	−261.5	−210.8	−265.0
225	−287.0	−355.1	−297.1	−256.2	−212.4	−335.6	−192.3	−156.7	−191.4
250	−221.0	−257.2	−220.5	−191.9	−159.5	−249.4	−147.3	−120.5	−144.2
275	−175.0	−195.8	−170.6	−149.3	−123.6	−193.4	−116.0	−94.6	−111.8
295	−147.1	—	—	—	—	—	—	—	—
300	−142.0	−154.1	−135.8	−119.1	−97.8	−154.5	−93.0	−75.4	−88.2
325	—	−124.2	−110.2	−96.8	−78.5	−126.0	−75.6	−60.5	−70.4
330	−114.0	—	—	—	—	—	—	—	—
350	—	−101.8	−90.7	−79.6	−63.4	−104.4	−61.9	−48.7	−56.5
370	−90.0	—	—	—	—	—	—	—	—
375	—	−84.5	−75.4	−66.0	−51.5	−87.4	−50.8	−39.1	−45.4
400	−76.0	−70.7	−63.0	−55.0	−42.8	−73.8	−41.7	−31.2	−36.3
420	−68.5	—	—	—	—	—	—	—	—
425	—	−59.5	−52.8	−45.9	−33.7	−62.6	−34.2	−24.6	−28.8
450	−59.0	−50.2	−44.4	−38.2	−26.9	−53.3	−27.8	−19.0	−22.4
475	—	−42.3	−37.2	−31.7	−21.2	−45.4	−22.3	−14.2	−17.0
480	−53.0	—	—	—	—	—	—	—	—

[a]Ref. 32.

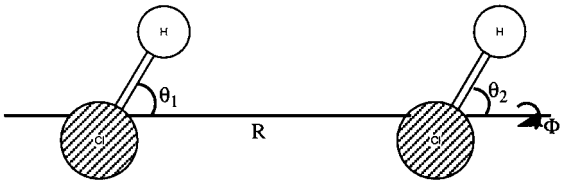

FIGURE 1. Reference system used for definition of geometry parameters describing the stationary points (*R* is the distance between the center of mass in the two molecules).

using a perturbation-based approach is of similar quality to those obtained using a supermolecular approach, despite the fact that the present approach requires for fewer computational resources.

References

1. S. Boys and F. Bernardi, *Mol. Phys.*, **19,** 558 (1970).
2. F. B. van Duijnefeldt, J. G. C. M. van Duijnefeldt-van de Rijdt, and J. H. van Lenthe, *Chem. Rev.*, **94,** 1873 (1994).
3. M. Gutowski, M. M. Szczesniak, and G. Chalasinski, *Chem. Phys. Lett.*, **241,** 140 (1995).
4. F.-M. Tao and W. Klemperer, *J. Chem. Phys.*, **103,** 950 (1995).
5. A. W. Meredith, Liu Ming, and S. Nordholm, *Chem. Phys.*, **220,** 63 (1997).
6. A. Wallqvist and G. Karlström, *Chem. Scr.*, **29A,** 131 (1989).
7. A. Wallqvist, P. Ahlström, and G. Karlström, *J. Phys. Chem.*, **94,** 1649 (1990).
8. P.-O. Åstrand, A. Wallqvist, and G. Karlström, *J. Chem. Phys.*, **95,** 8419 (1991).
9. P.-O. Åstrand, A. Wallqvist, and G. Karlström, *J. Chem. Phys.*, **100,** 1262 (1994).
10. G. Karlström, *Proceedings from the Fifth Seminar on Computational Methods in Quantum Chemistry*, Groningen, The Netherlands, 1981.
11. G. Karlström, P. Linse, A. Wallqvist, and B. Jönsson, *J. Am. Chem. Soc.*, **105,** 3777 (1983).
12. G. Karlström, *Theor. Chim. Acta*, **60,** 535 (1982).
13. C. Grey, and K. E. Gubbins, *Theory of Intermolecular Fluids*, Vol. 1, Clarendon, Oxford, 1984.
14. A. Karfen, P. R. Bunker, and P. Jensen, *Chem. Phys.*, **149,** 299 (1991).
15. C. Votava, R. Ahlrichs, and A. Geiger, *J. Chem. Phys.*, **78,** 6841 (1983).
16. P. R. Bunker, V. C. Epa, P. Jensen, and A. Karpfen, *J. Mol. Spectrosc.*, **149,** 299 (1991).
17. Z. Latajka and S. Scheiner, *Chem. Phys.*, **122,** 413 (1988).
18. J. S. Muenter, *J. Chem. Phys.*, **103,** 1263 (1995).
19. M. J. Elrod and R. J. Saykally, *J. Chem. Phys.*, **103,** 933 (1995).
20. (a) S. E. Novick, K. R. Leopold, and W. A. Klemperer, In *Atomic and Molecular Clusters*, E. R. Bernstein, Ed., Elsevier, New York, 1990; (b) A. S. Pine and B. J. Howard, *J. Chem. Phys.*, **84,** 590 (1986).
21. M. D. Schuder, C. M. Lovejoy, R. Lascola, and D. J. Nesbitt, *J. Chem. Phys.*, **99,** 4346 (1993).
22. K. Andersson, M. P. Fulscher, R. Lindh, P.-A. Malmqvist, J. Olsen, B. O. Roos, and A. Sadlej, *MOLCAS*-2, University of Lund, Sweden; P.-O. Widmark, IBM, Sweden, 1991.
23. K. Pierloot, B. Dumez, P.-O. Widmark, and B. Roos, *Theor. Chim. Acta*, **90,** 87 (1995).
24. A. J. Stone and M. Alderton, *Mol. Phys.*, **56,** 1047 (1985).
25. G. Karlström, *Theor. Chim. Acta*, **55,** 233 (1980).
26. T. K. Tang and J. P. Toennis, *J. Chem. Phys.*, **80,** 3726 (1984).
27. M. Margenau, and N. R. Kestner, *Theory of Intermolecular Forces*, Pergamon, Oxford, 1969.
28. A. J. Stone, *Am. Inst. Phys. Conf. Proc.*, **239,** 3 (1991).
29. G. Maroulis, *J. Phys.*, **24,** 117 (1991).
30. E. W. Kaiser, *J. Chem. Phys.*, **53,** 1686 (1970).
31. W. H. De Leeuw and A. J. Dymanus, *J. Mol. Spec.*, **48,** 427 (1973).
32. B. Schramm and U. Leuchs, *Ber. Bunsenges. Phys. Chem.*, **83,** 864 (1979).
33. J. G. Kirkwood, *J. Chem. Phys.*, **1,** 597 (1933).